AGU PUBLICATIONS

JGR

Journal of Geophysical Research: Space Physics

RESEARCH ARTICLE

10.1002/2013JA019593

Key Points:
- Clustering algorithms are applied to lightning data to locate thunderstorms
- Global electric circuit thunderstorm current is estimated from WWLLN
- A global average of 660 thunderstorms are estimated to produce 1090 A

Correspondence to:
M. L. Hutchins,
mlhutch@uw.edu

Citation:
Hutchins, M. L., R. H. Holzworth, and J. B. Brundell (2014), Diurnal variation of the global electric circuit from clustered thunderstorms, *J. Geophys. Res. Space Physics*, *119*, doi:10.1002/2013JA019593.

Received 4 NOV 2013
Accepted 8 JAN 2014
Accepted article online 14 JAN 2014

Diurnal variation of the global electric circuit from clustered thunderstorms

Michael L. Hutchins[1], Robert H. Holzworth[1], and James B. Brundell[2]

[1]Department of Earth and Space Sciences, University of Washington, Seattle, Washington, USA, [2]UltraMSK.com, Dunedin, New Zealand

Abstract The diurnal variation of the global electric circuit is investigated using the World Wide Lightning Location Network (WWLLN), which has been shown to identify nearly all thunderstorms (using WWLLN data from 2005). To create an estimate of global electric circuit activity, a clustering algorithm is applied to the WWLLN data set to identify global thunderstorms from 2010 to 2013. Annual, seasonal, and regional thunderstorm activity is investigated in this new WWLLN thunderstorm data set in order to estimate the source behavior of the global electric circuit. Through the clustering algorithm, the total number of active thunderstorms are counted every 30 min creating a measure of the global electric circuit source function. The thunderstorm clusters are compared to precipitation radar data from the Tropical Rainfall Measurement Mission satellite and with case studies of thunderstorm evolution. The clustering algorithm reveals an average of 660 $\pm$ 70 thunderstorms active at any given time with a peak-to-peak variation of 36%. The highest number of thunderstorms occurs in November (720 $\pm$ 90), and the lowest number occurs in January (610 $\pm$ 80). Thunderstorm cluster and electrified storm cloud activity are combined with thunderstorm overflight current measurements to estimate the global electric circuit thunderstorm contribution current to be 1090 $\pm$ 70 A with a variation of 24%. By utilizing the global coverage and high time resolution of WWLLN, the total active thunderstorm count and current is shown to be less than previous estimates based on compiled climatologies.

1. Introduction

Diurnal variation in global thunderstorm activity was original observed by *Wilson* [1921] and *Whipple* [1929] through a combination of thunderstorm day and electric field measurements. Strong correlations between thunderstorm activity and fair weather return current led to the model of the global electric circuit, a system of ionospheric charging and discharging through thunderstorms and fair weather return currents. Studies to date have estimated that globally there are 1000–2000 thunderstorms active at any one time, with most concentrated over tropical landmasses, covering 1–10% of Earth's surface [*Markson*, 1978; *Rycroft and Harrison*, 2011; *Singh et al.*, 2011]. Previous work on diagnosing the generator source of the global electric circuit used several methods: long time scales [*Tinsley et al.*, 2007; *Liu et al.*, 2010], mathematical models [*Kasemir*, 1977; *Hays and Roble*, 1979; *Roble*, 1991], engineering models [*Ogawa*, 1985; *Kartalev et al.*, 2004; *Rycroft*, 2006], parameterization [*Price and Rind*, 1992; *Williams*, 1985], and thunderstorm overflight estimates [*Mach et al.*, 2011]. Most work with the global electric circuit uses long-term averaging to recreate the known Carnegie curve of *Whipple* [1929], yet short time scales do not match the long-term averaging [*Holzworth et al.*, 1984]. The variation of the global electric circuit changes on short time scales that is not resolved in past models or with long-term averaged observations. The global electric circuit is an important component to the solar-terrestrial system creating a link between solar activity, the ionosphere, aerosols, cloud microphysics, thunderstorms, weather, and climate [*Tinsley et al.*, 2007; *Holzworth and Volland*, 1986].

Individual lightning strokes and flashes are not yet a reliable method of characterizing the source of the global electric circuit, but global thunderstorm activity is a reliable measure. *Ruhnke* [1969] proposes the Maxwell current above thunderstorms as the global electric circuit generator source as it varies slowly through the evolution of a thunderstorm and the current is fairly independent from impulsive events like lightning. *Krider and Blakeslee* [1985] looked at Maxwell currents below a thunderstorm to find them steady with abrupt, but insignificant, changes due to lightning. *Rycroft et al.* [2000] created an engineering model with three different regions for the return current, concluding that sprites, lightning, and other transients will have little direct effect on the global electric circuit. *Stergis et al.* [1957] showed that cloud to ground

lightning is not necessary for upward current from thunderstorms. With a numerical model of a dipolar thunderstorm *Tzur and Roble* [1985] estimated the upward current contribution of thunderstorms to the global electric circuit to be 0.7 A. Similarly, with a combination of numerical and analytical models of dipolar thunderstorm, *Driscoll et al.* [1992] estimated a total contribution of 0.4 A to the global circuit per thunderstorm. Unlike the other models, *Mareev et al.* [2008] estimated a 50–400 A current contribution directly from lightning; with a similar model *Mallios and Pasko* [2012] investigated the efficiency of lightning and found lightning contributed 1% of the total 300 A from thunderstorms. These works show that thunderstorms contribute an appreciable upward current to the global electric circuit independent of individual lightning strokes.

Balloon and aircraft overflights have been used to estimate the total current contributions from thunderstorms to the global electric circuit. *Stergis et al.* [1957] found thunderstorm currents ranging from 0.6 to 4.3 A, with an average of 1.3 A; these estimates are the lower bound with uncertainties of up to 50%. *Blakeslee et al.* [1989] show the upward current generated by a thunderstorm to range between 0.1 – 6 A with an average current between 0.5 and 1 A. Other studies show current density over thunderstorms ranging from 10 to 40 pA/km^2 [*Holzworth*, 1981], 40 to 70 pA/km^2 [*Rycroft*, 2006], and −20 to 33 nA/m^2 [*Mach et al.*, 2009]. The overflights in previous research found no consistent parameterization between lightning rates and fair weather return current, but recent balloon work found strong correlation between global lightning activity and the fair weather return current on short time scales [*Holzworth et al.*, 2005]. Lightning stroke activity and locations cannot directly provide estimates of the global circuit; however, they can be used for directly locating and defining active thunderstorm areas and relative intensities.

Compared to satellite and balloon observations, ground-based lightning networks have the advantage of continuous observation of large regions. Global very low frequency networks, such as the World Wide Lightning Location Network (WWLLN), are capable of locating lightning around the entire globe. *Holzworth et al.* [2005] compared the stroke counts of a nascent WWLLN to the fair weather return current and found strong temporal correlation between the measurements. A better measure of global circuit activity is the total number of active thunderstorms around the globe; applying clustering algorithms to lightning network data enables the network to locate, track, and monitor global thunderstorm activity.

The WWLLN (see http://wwlln.net/) is a global lightning network with, as of September 2013, over 70 VLF receivers distributed globally [*Rodger et al.*, 2006, 2009]. WWLLN locates strokes by analyzing the time of group arrival of the sferic wave packet in the 6–18 kHz band [*Dowden and Brundell*, 2000]. Previous studies have shown that WWLLN locates most strokes to an average accuracy of 10 km with a cloud to ground detection efficiency of 11% [*Rodger et al.*, 2009; *Abarca et al.*, 2010; *Hutchins et al.*, 2012a; *Rudlosky and Shea*, 2013]. A recent upgrade to the network allows for the measurement of the radiated VLF energy of located strokes within the 8–18 kHz VLF band [*Hutchins et al.*, 2012b]. Through comparisons with the Los Alamos Sferic Array *Jacobson et al.* [2006] found that WWLLN locates nearly all active thunderstorm regions.

The WWLLN data are clustered into thunderstorms with the Density-Based Spatial Clustering of Application with Noise (DBSCAN) algorithm [*Ester et al.*, 1996; *Kriegel et al.*, 2011]. DBSCAN was chosen as the clustering algorithm for several key features: the capability to handle noise, no requirement to specify the number of clusters, arbitrary cluster shapes, and the insensitivity to the ordering of the data. Clustering lightning strokes into thunderstorms cannot require a designated number of clusters before clustering, as the total number of thunderstorms is not known before clustering. Similar algorithms, such as Ward's method, cluster into large unphysical thunderstorms due to noise [*Ward*, 1963]. In another approach *Mezuman* [2013] used a connected component method to cluster the WWLLN data. They found global thunderstorm activity to average near 1000 thunderstorms with significant daily variability. The resulting WWLLN lightning clusters are representative of the lightning active stage of the thunderstorm. Even though the electrically active portion of a thunderstorm extends beyond the active lightning stage [*Jacobson and Krider*, 1976; *Stolzenburg et al.*, 2010], the clustered lightning active stage in this work will be referred to as the clustered thunderstorm or thunderstorm clusters.

2. Clustering

2.1. DBSCAN

DBSCAN clusters n-dimensional points based on the distance between the points, ϵ, and the minimum number of points necessary to form a cluster, *minPts* [*Kriegel et al.*, 2011]. Points in a cluster are either core

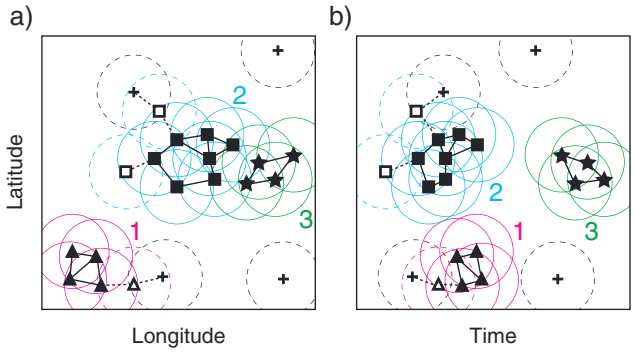

Figure 1. DBSCAN clustering example, with minPts = 3, showing the same clusters located in (a) latitude and longitude and (b) latitude and time. Solid rings show the ϵ distance from core points (filled), dashed rings are for noncore points (unfilled). Triangles (1), squares (2), and stars (3) show clustered points; crosses are nonclustered points.

points or noncore points. A point is a core point of a cluster if there are minPts −1 other points within ϵ distance of that point (resulting in minPts points within distance ϵ). In Figure 1 the distance ϵ is represented by the circle around each point, lines connect points within ϵ of each other, and core points are shown as filled symbols. Points that are within ϵ of one core point, but less than two core points (minPts = 3), are added to the cluster as noncore points and cannot be used to add more points into the cluster. For example, Figure 1 (unfilled triangle symbol in group 1) is within ϵ of one core point and clustered into the group as a noncore point but cannot connect further unclustered points (Figure 1, crosses) into the cluster.

WWLLN lightning strokes are separated by three dimensions: latitude, longitude, and time. With time as a consideration, two clusters that appear to overlap in Figure 1a (group 2 (blue) and group 3 (green)) are separated by ϵ in time and are distinct groups as seen in Figure 1b. DBSCAN is a physically realistic algorithm for clustering lightning data, such as WWLLN data, as the core points of a thunderstorm are the intense lightning centers, while edge points are clustered but do not connect disparate lightning centers.

2.2. Clustering WWLLN

Accurate thunderstorm clustering of WWLLN data requires optimizing the clustering parameters ϵ and minPts. WWLLN requires a second ϵ parameter, ϵ_{time}, for clustering in time. The parameter ϵ corresponds to the physical extent of an average thunderstorm, ϵ_{time} the duration, and minPts the number of lightning strokes necessary to consider a thunderstorm electrically active.

As the clustering parameters are varied the total number of thunderstorms, the average thunderstorm area, and the average thunderstorm duration change. In Figure 2a it can be seen that ϵ has a high degree of control over thunderstorm area and total thunderstorms. To balance the total number of thunderstorms, average area (320 km^2), and percentage of strokes clustered (89%, not shown) the best value is found to be $\epsilon = 0.12$. To prevent consecutive thunderstorms from being clustered (e.g., one thunderstorm occurring in the same area as a previous distinct thunderstorm storm) ϵ_{time}, Figure 2b, needs to be smaller than average duration of a thunderstorm. With this requirement the value of $\epsilon_{\text{time}} = 18$ min is found, giving an average thunderstorm cluster duration of 16 min. The minimum number of strokes needed to produce a cluster is set at minPts = 2, as two detected WWLLN strokes confirms the presence of a thunderstorm. A sharp drop in the total number of thunderstorms can be seen in Figure 2c when minPts moves from 2 to 3. To get a majority of strokes included in the thunderstorm clusters while retaining reasonable physical attributes of the thunderstorms the parameters $\epsilon = 0.12°$, $\epsilon_{\text{time}} = 18$ min, and minPts = 2 strokes were chosen.

3. WWLLN Thunderstorm Clusters

Using the DBSCAN algorithm, the individual WWLLN lightning strokes from June 2010 to June 2013 are clustered into active thunderstorms. Clustered WWLLN strokes allow for simple thunderstorm tracking as shown in Figure 3. Here the strokes comprising a thunderstorm are outlined with polygons every hour and plotted with opacity increasing with time. Figure 3 shows several active thunderstorms on 21 May 2013, 12–23 UTC. For clarity clustered thunderstorms with less than 50 strokes were removed from the plot. The thunderstorm opacity increases at 8% per hour with each color corresponding to a single thunderstorm cluster.

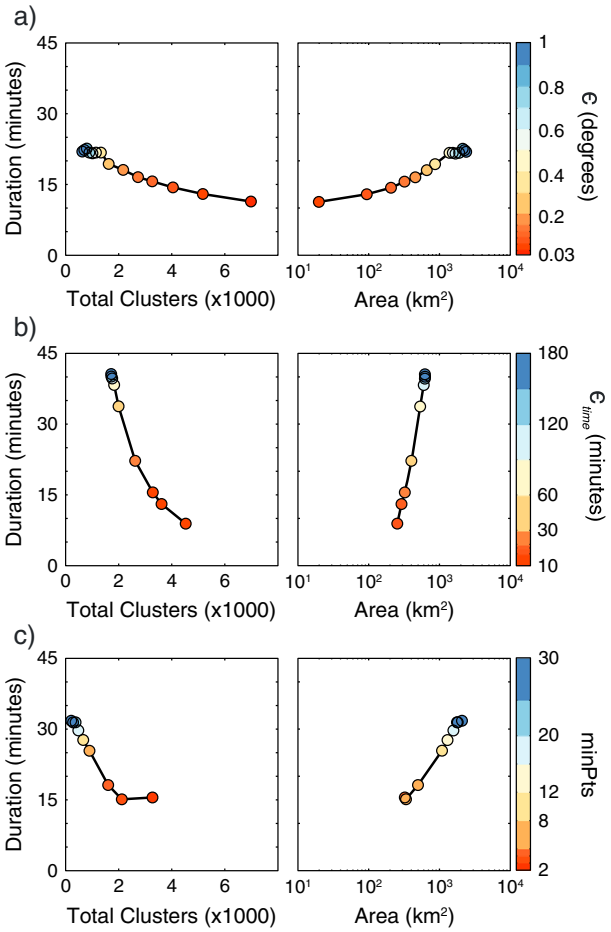

Figure 2. Variation in average thunderstorm duration (rows), counts (left column), and area (right column) through varying one clustering parameter with the others held constant (constant set: $\epsilon = 0.12^{\circ}$, $\epsilon_{time} = 18$ min, and minPts = 2); (a) ϵ varies from 0.03° to 1°; (b) ϵ_{time} varies from 10 to 180 min; and (c) minPts varies from 2 to 30 strokes.

The cluster results can be directly compared to active precipitation regions as seen by the Tropical Rainfall Measuring Mission (TRMM) Precipitation Radar [*Kawanishi et al.*, 2000]. Rainfall rates from the TRMM data product 2A25 were used as binned rates on a 0.25° grid. In Figure 4 the TRMM rainfall data are shown as the background image, gray areas are not in view of the satellite. WWLLN strokes are shown in Figure 4 if they occur between the start and end times of the TRMM regional overpass.

In Figure 4 two sets of consecutive overpasses are used: The first is on 6 May 2013 from 15:49–15:59 UTC (Figure 4a) to 17:28–17:37 UTC (Figure 4b), and the second is on 21 May 2013 from 10:04–10:13 UTC (Figure 4c) to 11:42–11:52 UTC (Figure 4d). These passes were selected as they passed over the same thunderstorms twice with an appreciable amount of lightning activity in view of the satellite. Unlike Figure 3, the clustered WWLLN strokes are shown as individual strokes in the thunderstorm with many of the strokes overlapping each other in the center of the clustered regions. The clustered thunderstorms match up well with the TRMM precipitation regions and clearly track the same thunderstorm between the consecutive overpasses. Thunderstorms continue and are clustered by WWLLN, well after TRMM no longer observes the area (Figures 4c and 4d, green thunderstorm). There were no previous or later TRMM overpasses of these thunderstorms.

4. Global Thunderstorm Activity

Original estimates of global thunderstorm activity show afternoon peaks in lightning activity for each of the major lightning chimney regions: the Americas, Africa/Europe, and Asia [*Wilson*, 1921]. The global averaged WWLLN thunderstorm clusters show the previously measured long-term averaged diurnal behavior of the global electric circuit activity, with a diurnal variation of 36%. The 3 year average of thunderstorm activity is shown in Figure 5 for different regions (Figure 5a), for thunderstorm type (Figure 5b), and for seasons (Figure 5c), with the global average displayed in each panel (Figure 5, black). Averages of thunderstorm activity are calculated from the total number of unique thunderstorms every 30 min.

Each chimney region is separated in Figure 5a with peaks in thunderstorm activity occurring in the local afternoon (Americas 19 UTC, Africa 15 UTC, and Asia 8 UTC) with a slow decrease during the night until a minimum in the early hours of the morning. A strong diurnal variation is evident for thunderstorms over land, seen in Figure 5b, with little diurnal variation in oceanic thunderstorm activity. On average WWLLN observes a total of 660 $\pm$ 70 thunderstorms on any given day of the year. While the total is lower than previous estimates in the 1000–2000 thunderstorm range, those estimates were made using partial or extrapolated data sets. For each chimney region the average number of thunderstorms are 280 $\pm$ 80 for the Americas, 140 $\pm$ 60 for African and Europe, and 240 $\pm$ 50 for Asia and the Maritime Continent. The long-term thunderstorm behavior observed by WWLLN resembles the previous measurement of global electric circuit

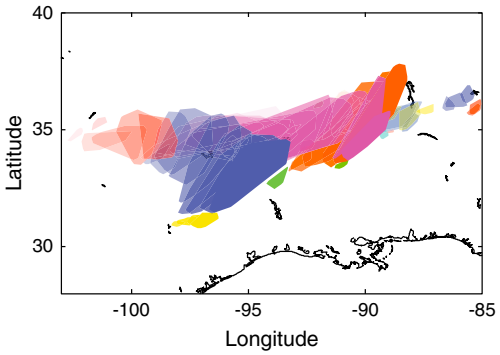

Figure 3. Thunderstorm evolution from 21 May 2013, 12–23 UTC. Polygons outline active lightning regions, colors correspond to thunderstorm cluster, opacity increases 8%/h. For clarity, thunderstorms with less than 50 strokes were removed.

behavior. Of the clustered thunderstorms 350 ± 70 were continental and 300 ± 10 were oceanic. This is in contrast to the disparity in the distribution of individual lightning strokes where a majority are continental; the continental thunderstorms tend to be larger with higher stroke rates than those over the oceans.

There are slight changes in the overall diurnal behavior between each season shown Figure 5c. The contribution of each chimney region, divided by Northern and Southern Hemisphere, is shown in Figure 6. The overall seasonal change in thunderstorm activity is clearly seen with the change in dominant contributor from the Northern Hemisphere in May–August to the Southern Hemisphere in November–February. In the shoulder seasons (March–April and September–October) the different chimney are closer in activity levels to each other. The shift in peak activity times for each chimney region between northern and southern summer reflects the difference in longitudinal landmass distribution of each region. For example the North America peak occurs at 23:30 UTC, while the South America peak occurs at 18:30 UTC since the South American lightning regions are, in general, farther east than the North American ones. This time change in regional contributions has been seen in other global circuit measurements; in the Vostok, Antarctica, electric field measurements of the fair weather field, the peak in field strength changes from 18:00 UTC in January to 21:00 UTC in August [*Burns et al.*, 2005, 2012].

5. Temporal Thunderstorm Activity

As a result of constantly growing number of WWLLN stations, the number of WWLLN strokes detected increases with time due to improvements in the network and the detection efficiency. As a result long-term tracking of stroke rate cannot be used without deconvolving detection efficiency improvements. However, thunderstorm counts have remained relatively constant while stroke rate has increased; WWLLN has been capable of detecting almost every thunderstorm since 2005 [*Jacobson et al.*, 2006]. In Figure 7a the daily average 30 min thunderstorm counts (Figure 7, black) are plotted alongside the daily average stroke rate

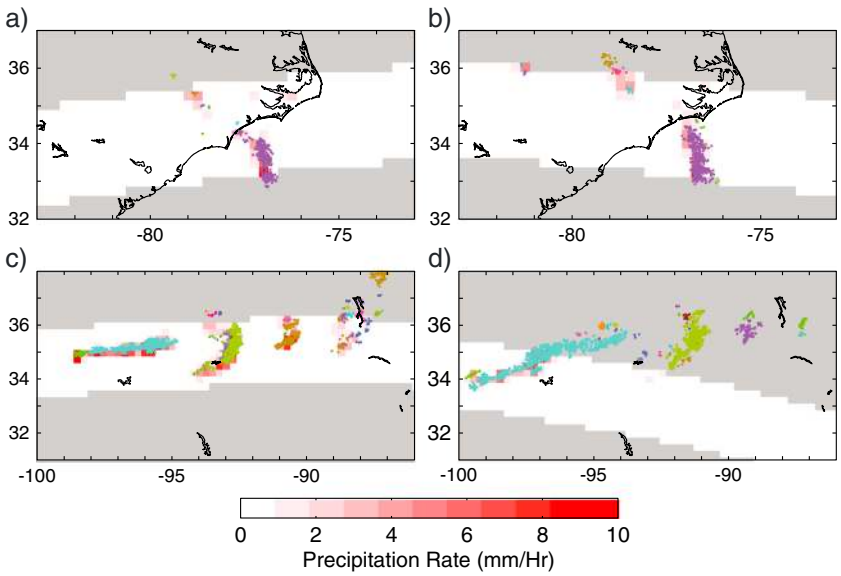

Figure 4. WWLLN thunderstorm clusters (identified by color) over TRMM precipitation rate (mm/h) for 6 May 2013, (a) 15:49–15:59 UTC, (b) 17:28–17:37 UTC, and 21 May 2013, (c) 10:04–10:13 UTC, (d) 11:42–11:52 UTC. Figures 4a and 4b are successive passes as are Figures 4c and 4d; cluster colors are contiguous between passes. Gray areas were outside the range of the TRMM radar.

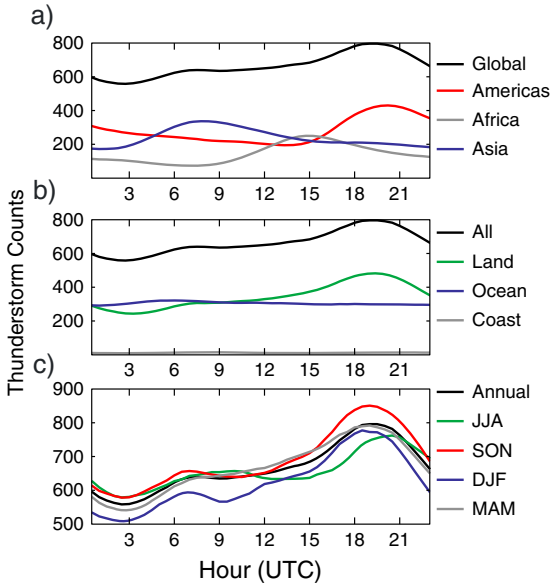

Figure 5. Diurnal variation of WWLLN thunderstorm 30 min counts for 2010–2013 obtained using the DBSCAN clustering algorithm. (a) Thunderstorms over each major lightning chimney region (divided between longitudes −180°, −30°, and 60°), (b) all, land, ocean, and coastal thunderstorms (coastal thunderstorms have strokes over land and ocean), and (c) the full year and each season.

(Figure 7, red). It can been seen that the stroke rate has increased relatively steadily, while the thunderstorm count has remained relatively stable.

The daily average thunderstorm count remains relatively constant during 2010–2013, while the stroke rate increases during the same time span. The thunderstorm count increased an average of 3% per year, while the stroke had a much higher yearly increase of 13%. Similarly, 90% of the daily thunderstorm averages are within 20% of the mean for the 3 years. Previous work has suggested that changes in climate will cause a change in global thunderstorm behavior [*Williams*, 2005; *Price*, 2009]. During 2010–2013 the average global surface temperature and thunderstorm count have both remained relatively constant [*Hansen et al.*, 2013], but future changes in global temperature may be reflected in the global average thunderstorm count.

Figure 8 shows that the typical diurnal behavior of Figure 5 emerges only after long-term averaging. When examining the thunderstorm counts on a monthly scale (Figure 8, dash-dotted line) the long-term average begins to emerge, while over a single day (Figure 8, dashed line), the expected diurnal behavior is missing. Similarly, on the daily scale of Figure 7c it can be seen clearly that stroke rate does not follow thunderstorm counts as located by WWLLN. Despite the short time scale variation, the overall average of the data still accurately reproduces the expected global thunderstorm activity in Figure 5. With such short time scale variation global observations

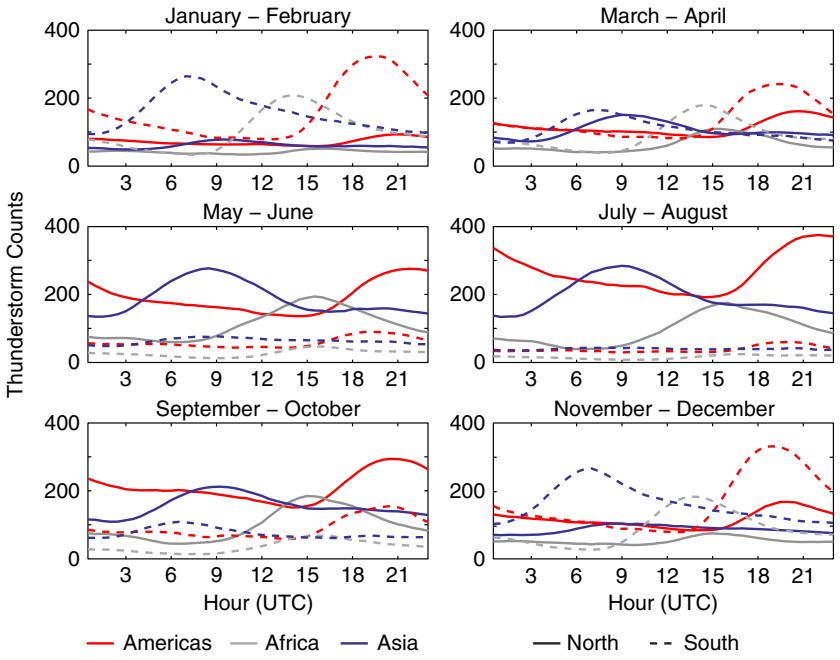

Figure 6. Diurnal variation of WWLLN thunderstorms for each major chimney region (colors) divided by hemisphere (Northern Hemisphere: solid line and Southern Hemisphere: dashed line). Each panel shows 2 months of thunderstorm clusters averaged over 2010–2013.

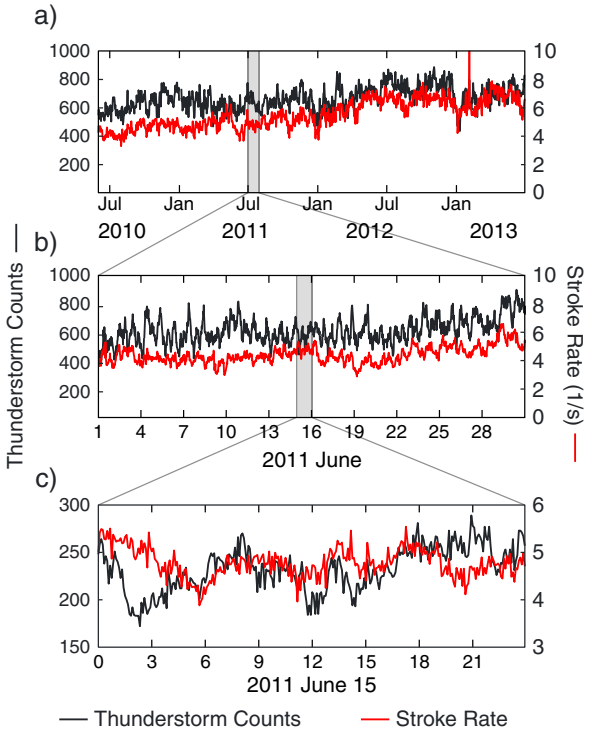

Figure 7. Variation in WWLLN thunderstorm count (black) and stroke rate (red) for (a) daily averages 30 min counts from June 2010 to June 2013, (b) 30 min counts from 1 to 30 June 2011, and (c) 5 min counts from 15 June 2011, 00–23 UTC.

of the global electric circuit source mechanism, be it with ground lightning networks or several geostationary satellites, needs to occur along with an accurate measure of the return current to better understand the charging of the global electric circuit.

6. Global Electric Circuit Thunderstorm Contribution

With the WWLLN thunderstorm clusters a simple model is made to estimate the total contribution of thunderstorms and electrified storm clouds to the global electric circuit. *Mach et al.* [2011] considered Lightning Imaging Sensor and Optical Transient Detector (LIS/OTD) observed land thunderstorms with less than 1.7 flashes min^{-1} and ocean thunderstorms with less than 0.33 flashes min^{-1} electrified storm clouds. For an average storm duration of 15 min these cutoffs are 26 flashes for land and 5 flashes for oceanic electrified storm clouds (ESCs). With a WWLLN-LIS/OTD detection efficiency of 6.4% over land and 17% over oceans [*Rudlosky and Shea*, 2013], WWLLN would expect cutoffs of two strokes per thunderstorm over land and one stroke per thunderstorm over oceans. Given the clustering parameters used in this work requires a minimum of two strokes to be considered a thunderstorm, every unclustered WWLLN stroke is considered a single ESC. The daily average of thunderstorms and ESCs observed by WWLLN are shown in Figure 9a. Since not all ESC will produce lightning the counts shown in Figure 9a should be considered a low estimate.

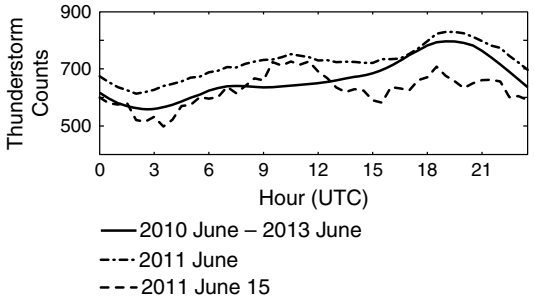

Figure 8. Diurnal UTC variation in WWLLN 30 min thunderstorm count for multiyear average of Figure 7a (solid line), monthly average of Figure 7b (dash-dotted line), and 30 min averages of Figure 7c (dashed line).

The average thunderstorm and ESC current contribution is taken from the overflight data of *Mach et al.* [2010]. Average current contribution for land thunderstorms is 1.0 A, for oceanic thunderstorms 1.7 A, for land ESCs 0.41 A, and

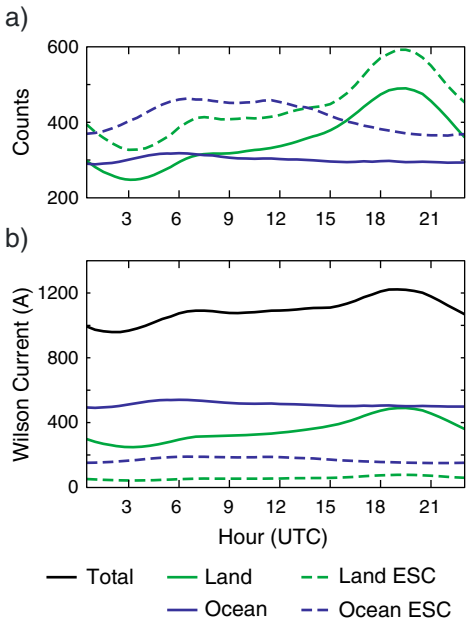

Figure 9. A simple model of the total global electric circuit current with contributions from land thunderstorms (green solid line), oceanic thunderstorms (blue solid line), land electrified storm clouds (green dashed line), and oceanic electrified storm clouds (blue dashed line). (a) The counts for each group and b) the current contribution to the total (black line).

for oceanic ESCs 0.13 A. The total current for each contributor and the total current is shown in Figure 9b. The average thunderstorm current is found to be 1090 ± 70 A with a total peak-to-peak variability of 24%. The largest contributor are oceanic thunderstorms (47%) with 510 ± 10 A, followed by land thunderstorms (32%) with 350 ± 70 A. Overall ESCs contribute 21% to the thunderstorm global circuit current.

With a similar model based on the TRMM LIS/OTD data, *Mach et al.* [2011] found that ocean thunderstorms contribute 32% and land thunderstorms 55%, with a total ESC contribution of 13% to the total mean current of 2.04 kA. Their difference in current and contributor fraction stems from an increased count of land thunderstorms. This highlights a shortcoming of this simple model, land thunderstorms tend to be larger than oceanic storms; thunderstorm area should be taken into account along with overall counts. However, to validate any global circuit model a comparison needs to be made with simultaneous fair weather return current measurements in order to constrain the models.

7. Conclusion

Global thunderstorm count is a good measure of global electric circuit activity and for a simple model of the circuit; the location and size of thunderstorms are necessary along with totals to create a more accurate model of the real-time fair weather return current. WWLLN strokes are successfully clustered into thunderstorms using the DBSCAN clustering algorithm with appropriately chosen clustering parameters. The clustered thunderstorms were compared against the TRMM Precipitation Radar and a case study of thunderstorm tracking and evolution. When the 3 years of WWLLN data were averaged the diurnal behavior of global thunderstorm activity aligned with the expected behavior of both thunderstorms and the fair weather return current. The results of global thunderstorm and electrified storm cloud activity are combined with upward thunderstorm current averages to create an estimate of the fair weather return current. The model found an average thunderstorm current contribution of 1090 ± 70 A. This and future, estimates of the current can be validated against an accurate fair weather return current measurement.

Acknowledgments

The authors wish to thank the World Wide Lightning Location Network (http://wwlln.net), a collaboration among over 50 universities and institutions for providing lightning location data used in this paper. The TRMM data used in this effort were acquired as part of the activities of NASA's Science Mission Directorate and are archived and distributed by the Goddard Earth Sciences (GES) Data and Information Services Center (DISC).

Robert Lysak thanks Brian Tinsley and an anonymous reviewer for their assistance in evaluating this paper.

References

Abarca, S. F., K. L. Corbosiero, and T. J. Galarneau (2010), An evaluation of the Worldwide Lightning Location Letwork (WWLLN) using the National Lightning Detection Network (NLDN) as ground truth, *J. Geophys. Res.*, *115*, D18206, doi:10.1029/2009JD013411.

Blakeslee, R. J., H. J. Christian, and B. Vonnegut (1989), Electrical measurements over thunderstorms, *J. Geophys. Res.*, *94*(89), 13,135–13,140.

Burns, G. B., A. Frank-Kamenetsky, O. A. Troshichev, E. A. Bering, and B. D. Reddell (2005), Interannual consistency of bi-monthly differences in diurnal variations of the ground-level, vertical electric field, *J. Geophys. Res.*, *110*, D10106, doi:10.1029/2004JD005469.

Burns, G. B., B. A. Tinsley, A. V. Frank-Kamenetsky, O. A. Troshichev, W. J. R. French, and A. R. Klekociuk (2012), Monthly diurnal global atmospheric circuit estimates derived from Vostok electric field measurements adjusted for local meteorological and solar wind influences, *J. Atmos. Sci.*, *69*(6), 2061–2082, doi:10.1175/JAS-D-11-0212.1.

Dowden, R. L., and J. B Brundell (2000), Improvements relating to the location of lightning discharges.

Driscoll, K. T., R. J. Blakeslee, and M. E. Baginski (1992), A modeling study of the time-averaged electric currents in the vicinity of isolated thunderstorms, *J. Geophys. Res.*, *97*(D11), 11,535–11,551.

Ester, M., H. Kriegel, J. Sander, and X. Xu (1996), A density-based algorithm for discovering clusters in large spatial databases with noise, in *2nd International Conference on Knowledge Discovery and Data Mining, KDD, 96*, 226–231.

Hansen, J., M. Sato, and R. Ruedy (2013), Global temperature update through 2012. [Available at www.nasa.gov/pdf/719139main _2012_GISTEMP_summary.pdf.]

Hays, P. B., and R. G. Roble (1979), A quasi-static model of global atmsopheric electricity 1. The lower atmosphere, *J. Geophys. Res.*, *84*(A7), 3291–3305.

Holzworth, R. (1981), High latitude stratospheric electrical measurements in fair and foul weather under various solar conditions, *J. Atmos. Terr. Phys.*, *43*(11), 1115–1125.

Holzworth, R., and H. Volland (1986), Do we need a geoelectric index?, *Eos Trans. AGU*, *67*(26), 545–548.

Holzworth, R., T. Onsager, P. Kintner, and S. Powerll (1984), Planetary-scale variability of the fair-weather vertical electric field in the stratosphere, *Phys. Rev. Lett.*, *53*(14), 1398–1401.

Holzworth, R. H., et al. (2005), Balloon observations of temporal variation in the global circuit compared to global lightning activity, *Adv. Space Res.*, *36*, 2223–2228.

Hutchins, M. L., R. H. Holzworth, J. B. Brundell, and C. J. Rodger (2012a), Relative detection efficiency of the World Wide Lightning Location Network, *Radio Sci.*, *47*, RS6005, doi:10.1029/2012RS005049.

Hutchins, M. L., R. H. Holzworth, C. J. Rodger, and J. B. Brundell (2012b), Far-field power of lightning strokes as measured by the World Wide Lightning Location Network, *J. Atmos. Oceanic Technol.*, *29*(8), 1102–1110, doi:10.1175/JTECH-D-11-00174.1.

Jacobson, A. R., R. Holzworth, J. Harlin, R. Dowden, and E. Lay (2006), Performance assessment of the World Wide Lightning Location Network (WWLLN), using the Los Alamos Sferic Array (LASA) as ground truth, *J. Atmos. Oceanic Technol.*, *23*(8), 1082–1092, doi:10.1175/JTECH1902.1.

Jacobson, E., and E. Krider (1976), Electrostatic field changes produced by Florida lightning, *J. Atmos. Sci.*, *33*, 103–117.

Kartalev, M., M. Rycroft, and V. Papitashvili (2004), A quantitative model of the effect of global thunderstorms on the global distribution of ionospheric electrostatic potential, *J. Atmos. Sol. Terr. Phys.*, *66*(13–14), 1233–1240, doi:10.1016/j.jastp.2004.05.012.

Kasemir, H. W. (1977), Theoretical problems of the global atmospheric electric circuit, in *Electrical Processes in Atmospheres*, edited by H. Dolezalek and R. Reiter, pp. 423–439, Steinkopff, Darmstadt.

Kawanishi, T., H. Kuroiwa, M. Kojima, K. Oikawa, T. Kozu, H. Kumagai, K. Okamoto, M. Okumura, H. Nakatsuka, and K. Nishikawa (2000), TRMM precipitation radar, *Adv. Space Res.*, *25*(5), 969–972.

Krider, E. P. I., and R. J. Blakeslee (1985), The electric currents produced by thunderclouds, *J. Electrostat.*, *16*, 369–378.

Kriegel, H.-P., P. Kröger, J. Sander, and A. Zimek (2011), Density-based clustering, *Wiley Interdiscip. Rev. Data Min. Knowl. Discovery*, *1*(3), 231–240, doi:10.1002/widm.30.

Liu, C., E. R. Williams, E. J. Zipser, and G. Burns (2010), Diurnal variations of global thunderstorms and electrified shower clouds and their contribution to the global electrical circuit, *J. Atmos. Sci.*, *67*(2), 309, doi:10.1175/2009JAS3248.1.

Mach, D. M., R. J. Blakeslee, M. G. Bateman, and J. C. Bailey (2009), Electric fields, conductivity, and estimated currents from aircraft overflights of electrified clouds, *J.Geophys. Res.*, *114*, 1–15, doi:10.1029/2008JD011495.

Mach, D. M., R. J. Blakeslee, M. G. Bateman, and J. C. Bailey (2010), Comparisons of total currents based on storm location, polarity, and flash rates derived from high-altitude aircraft overflights, *J. Geophys. Res.*, *115*, D03201, doi:10.1029/2009JD012240.

Mach, D. M., R. J. Blakeslee, and M. G. Bateman (2011), Global electric circuit implications of combined aircraft storm electric current measurements and satellite-based diurnal lightning statistics, *J. Geophys. Res.*, *116*, D05201, doi:10.1029/2010JD014462.

Mallios, S. A., and V. P. Pasko (2012), Charge transfer to the ionosphere and to the ground during thunderstorms, *J. Geophys. Res.*, *117*, A08303, doi:10.1029/2011JA017061.

Mareev, E. A., S. A. Yashunin, S. S. Davydenko, T. C. Marshall, M. Stolzenburg, and C. R. Maggio (2008), On the role of transient currents in the global electric circuit, *Geophys. Res. Lett.*, *35*(15), L15810, doi:10.1029/2008GL034554.

Markson, R. (1978), Solar modulation of atmospheric electrification and possible implications for the Sun-weather relationship, *Nature*, *273*, 103–109.

Mezuman, K. (2013), Detecting global thunderstorm distribution from lightning clusters, MSc thesis, Tel Aviv Univ., Tel Aviv, Israel.

Ogawa, T. (1985), Fair-weather electricity, *J. Geophys. Res.*, *90*(10), 5951–5960.

Price, C. (2009), Will a drier climate result in more lightning?, *Atmos. Res.*, *91*(2-4), 479–484, doi:10.1016/j.atmosres.2008.05.016.

Price, C., and D. Rind (1992), A simple lightning parameterization for calculating global lightning distributions, *J. Geophys. Res.*, *97*(D9), 9919–9933.

Roble, R. (1991), On modeling component processes in the Earth's global electric circuit, *J. Atmos. Terr. Phys.*, *53*(9), 831–847, doi:10.1016/0021-9169(91)90097-Q.

Rodger, C. J., S. Werner, J. B. Brundell, E. H. Lay, N. R. Thomson, R. H. Holzworth, and R. L. Dowden (2006), Detection efficiency of the VLF World-Wide Lightning Location Network (WWLLN): Initial case study, *Ann. Geophys.*, *24*, 3197–3214.

Rodger, C. J., J. B. Brundell, R. H. Holzworth, E. H. Lay, N. B. Crosby, T.-Y. Huang, and M. J. Rycroft (2009), Growing detection efficiency of the World Wide Lightning Location Network, *AIP Conf. Proc.*, *1118*, 15–20, doi:10.1063/1.3137706.

Rudlosky, S. D. S., and D. T. D. Shea (2013), Evaluating WWLLN performance relative to TRMM/LIS, *Geophys. Res. Lett.*, *40*, 1–5, doi:10.1002/grl.50428.

Ruhnke, L. (1969), Area averaging of atmospheric electric currents, *Tech. Rep. 1*, Atmospheric Physics and Chemistry Lab., Boulder, Colo.

Rycroft, M. J. (2006), Electrical processes coupling the atmosphere and ionosphere: An overview, *J. Atmos. Sol. Terr. Phys.*, *68*(3–5), 445–456, doi:10.1016/j.jastp.2005.04.009.

Rycroft, M. J., and R. G. Harrison (2011), Electromagnetic atmosphere-plasma coupling: The global atmospheric electric circuit, *Space Sci. Rev.*, *168*(1–4), 363–384, doi:10.1007/s11214-011-9830-8.

Rycroft, M. J., S. Israelsson, and C. Price (2000), The global atmospheric electric circuit, solar activity and climate change, *J. Atmos. Sol. Terr. Phys.*, *62*(17–18), 1563–1576, doi:10.1016/S1364-6826(00)00112-7.

Singh, A. K., D. Siingh, R. P. Singh, and S. Mishra (2011), Electrodynamical coupling of Earth's atmosphere and ionosphere: An overview, *Int. J. Geophys.*, *2011*, 1–13, doi:10.1155/2011/971302.

Stergis, C. G., G. C. Rein, and T. Kangas (1957), Electric field measurements above thunderstorms, *J. Atmos. Sol. Terr. Phys.*, *11*, 83–90.

Stolzenburg, M., T. C. Marshall, and P. R. Krehbiel (2010), Duration and extent of large electric fields in a thunderstorm anvil cloud after the last lightning, *J. Geophys. Res.*, *115*, D19202, doi:10.1029/2010JD014057.

Tinsley, B., G. Burns, and L. Zhou (2007), The role of the global electric circuit in solar and internal forcing of clouds and climate, *Adv. Space Res.*, *40*, 1126–1139, doi:10.1016/j.asr.2007.01.071.

Tzur, I., and R. Roble (1985), The interaction of a dipolar thunderstorm with its global electrical environment, *J. Geophys. Res.*, *90*(D4), 5989–5999.

Ward, J. H. J. (1963), Hierarchical grouping to optimize an objective function, *J. Am. Stat. Assoc.*, *58*(301), 236–244.

Whipple, F. (1929), On the association of the diurnal variation of electric potential gradient in fine weather with the distribution of thunderstorms over the globe, *Q. J. R. Meteorolog. Soc.*, *55*(229), 1–18.

Williams, E. R. (1985), Large-scale charge separation in thunderclouds, *J. Geophys. Res.*, *90*(D4), 6013–6025.

Williams, E. R. (2005), Lightning and climate: A review, *Atmos. Res.*, *76*, 272–287.

Wilson, C. T. R. (1921), Investigation on lightning discharges and on the electric field of thunderstorms, *Philos. Trans. R. Soc. London*, *221* (1921), 73–115.